GROWTH AND ELECTRICAL PROPERTIES OF (La,Sr)CoO₃/ Pb(Zr,Ti)O₃/(La,Sr)CoO₃ HETEROSTRUCTURES FOR FIELD EFFECT TRANSISTOR

J. Lee and S. W. Kim

Department of Materials Engineering, Sung Kyun Kwan University, Suwon, 440-746, Korea

ABSTRACT

Epitaxial (La, Sr)CoO₃/Pb(Zr, Ti)O₃/(La, Sr)CoO₃ heterostructures have been successfully grown on LaAlO₂ by pulsed laser deposition for ferroelectric field effect transistor. Epitaxial LaCoO₃/Pb(Zr, Ti)O₃/(La, Sr)CoO₃ heterostructures exhibited $70\mu C/cm^2$ and $17\mu C/cm^2$ at a positively and negatively poled states, respectively. On the other hand, epitaxial (La, Sr)CoO₃/Pb (Zr, Ti)O₃/LaCoO₃ heterostructures show the remnant polarization states opposite to the LaCoO₃/Pb(Zr, Ti)O₃/(La, Sr)CoO₃ heterostructures. This indicates that the interface between (La, Sr)CoO₃ (LSCO) and Pb(Zr, Ti)O₃ (PZT) layers affects the asymmetric polarization remanence through electrochemical nature. The resistivity of LaCoO₃ (LCO) layer was found to be dependent on an ambient oxygen, primarily the ambient oxygen pressure during deposition. The resistivity of the LCO layer varied in the range of 0.1-100 Ωcm. It is suggested that, with an appropriate resistivity of the LCO layer, the LCO/PZT/LSCO heterostructure can be used as the ferroelectric field effect transistor.

INTRODUCTION

Ferroelectric thin films have received great attention primarily due to memory device applications.[6-10] Several important characteristics inherent in ferroelectric materials such as remnant polarization and high dielectric constant are used in non-volatile memories and dynamic random access memories (DRAM), respectively. Various efforts for the realization of the memory device are currently directed at producing reliable ferroelectric thin film capacitors incorporated into the complementary metal-oxide semiconductor (CMOS) based integrated circuits. Among the memory devices, non-volatile ferroelectric memories have two differ-

ent type of read operation modes, i.e., destructive readout (DRO) and non-destructive readout (NDRO). To date, non-volatile ferroelectric memory with destructive readout mode are extensively studied. These devices undergo a large amount of read/ write cycles when used with a destructive readout mode in order to dynamically retrieve/store information and thus are required to have long-term reliability under various operating conditions such as fatigue, retention and imprint. Hence, the main emphasis on research for the realization of a commercially viable ferroelectric memory has been on processing of the ferroelectric thin films compatible with CMOS processing and reliable performance of fer-

roelectric capacitors.[5-6]

On the other hand, the non-volatile memory with non-destructive readout mode employs the same structure as field effect transistor, in which the conventional gate oxide is replaced by ferroelectric material. The ferroelectric field effect induces the compensation charges in Si and thus the modulation of conductance in Si. As a result, the ferroelectric material as a gate oxide provides the transistor with the non-destructive readout mode as well as non-volatility.

This ferroelectric field effect transistor (FEFET) alleviates the stringent requirement of the long-term reliability (i.e., fatigue) on the ferroelectric material, compared with the non-volatile memory with the destructive readout mode. Despite of various advantages of FEFET, reliable performance of FEFET was hindered by great difficulty in fabricating ferroelectric thin film directly on Si and charge injection between the ferroelectric thin film and Si.[11,12] The interface between the ferroelectric thin film and Si is easily degraded by interdiffusion or reaction of the ferroelectric oxide thin film and Si. Recently, ferroelectric field effect on conducting oxide such as $SrCuO_2$[13] and $(La, Sr)_2CuO_4$[14] has been reported

In this study, we have used an conducting oxide $((La, Sr)CoO_3)$ as a conducting channel instead of Si. $Pb(Zr, Ti)O_3$ (PZT) is used as a ferroelectric layer. It is expected that the interface between ferroelectric layer and the conducting channel layer is improved mainly due to the junction of oxide layers. Several characteristics of ferroelectric oxide layer and conducting oxide

channel layer have to be investigated. Ferroelectric properties of the PZT layer such as remnant polarization and polarization switching behavior affect the modulation of resistance in the conducting channel layer. First of all, heteroepitaxial $(La, Sr)CoO_3/Pb(Zr, Ti)O_3/(La, Sr)CoO_3$ heterostructure with all epitaxial nature have been grown to obtain high quality interface between PZT and $(La, Sr)CoO_3$ (LSCO) layers. The ferroelectric properties of the multilayers and the resistivity of the conducting oxide channel layer are investigated. This paper presents the results of the growth and the electrical properties of the heterostructures.

EXPERIMENTAL PROCEDURE

PZT and LSCO layers have been grown on $LaAlO_3$ substrate by pulsed Nd:YAG laser deposition. For the growth of epitaxial LSCO/PZT/LSCO heterostructures, $LaAlO_3$ was used a substrate. The LSCO layer was first grown on the $LaAlO_3$ substrate and $Pb(Zr,Ti)O_3$ (PZT) thin films were further deposited on the LSCO layer. Subsequently, $LaCoO_3$ (LCO) was deposited on the PZT/LSCO heterostructure. In the LCO/PZT/LSCO heterostructure, the bottom LSCO layer is used as an electrode while the top LCO layer is used as a channel layer.$(La_{0.5}Sr_{0.5})CoO_3$ sintered target was used for the deposition of the bottom LSCO layer in order to obtain high conductivity. For the deposition of LCO channel layer, $LaCoO_3$ sintered target was used in order to have appropriate charge carrier concentration. $Pb(Zr_{0.52}Ti_{0.48})O_3$ sintered ceramic targets were used For the deposition of PZT films. All the layer in the heterostructure were deposited at

substrateX temperatures of 550-750℃ and at an ambient oxygen pressure of 100-300 mTorr. The epitaxial growth of the heterostructure was examined by x-ray θ-2θ scan and ψ scan (pole figure measurement). The samples were first aligned to diffract the (204) plane and were rotated about an axis normal to the substrate surface. The direction, in which maximum intensity was obtained, was set to zero degree. The samples were then positioned to diffract incident x-ray from the{110} planes of the LSCO films and were rotated about an axis normal to the substrate plane.

This scan was repeated for the PZT films. For the electrical measurements, test capacitors with Pt/Au contact pads and dots of 100μm diameter on the LSCO top electrodes were delineated by a photolithographic lift-off process. The Pt/Au dots were subsequently used as a mask for etching the uncovered top LSCO layer with a 1% nitric acid solution to achieve electrical isolation of each capacitor. Contact to the bottom electrode was achieved by capacitive coupling from a large contact on the wafer. Ferroelectric properties of the heterostructure were measured using a Radiant Technologies pulsed testing system (RT66A). First, ferroelectric hysteresis loop and pulse polarization measurements for ferroelectric properties were carried out using a single triangle wave and a series of pulses, respectively. In the hysteresis loop measurement, the measuring voltage begins at 0 volts and steps in discrete voltage intervals (200 mV) to the assigned maximum voltages (Vmax) with the time increment of 100 μsec, then back to 0 volts, then to-Vmax, and then back to 0

volts. The sheet resistances of LSCO layers were measured by the four point (square or linear geometry) probe method. The applied source current was in range of 10^{-7} to 10^{-4} A.

RESULTS AND DISCUSSION

Figure 1 shows X-ray diffraction patterns of $(La_{0.5}Sr_{0.5})CoO_3$ (LSCO) thin films deposited on $LaAlO_3$ substrate. Perovskite LSCO thin films were obtained with highly oriented nature at substrate temperatures of 600℃ to 700℃. The ambient oxygen pressure was 200 mTorr at the deposition. It is well known that the underlying conducting oxide layer affects the characteristics of further growing perovskite PZT layer such as the composition of the PZT layer, the formation of perovskite structure and the orientation of the perovskite PZT layer. This LSCO layer will assist the formation of the perovskite PZT layer and furthermore the highly oriented nature of the LSCO layer affects the orientation of
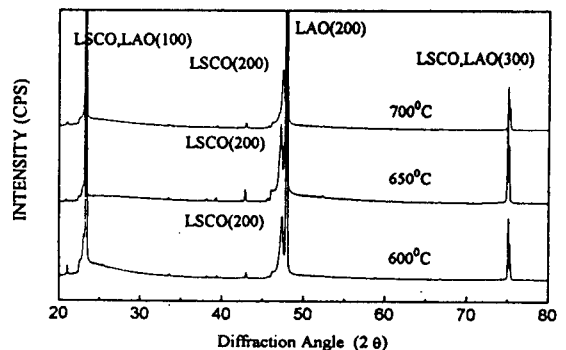

Fig. 1. X-ray diffraction patterns of $(La_{0.5}Sr_{0.5})CoO_3$ (LSCO) thin films deposited at substrate temperatrues of 600-700℃ on $LaAlO_3$ substrate.

the perovskite PZT layer. The oxygen ambient during the deposition of LSCO layers was varied while substrate temperature was maintained at 650℃ for the depositions. Figure 2 shows x-ray diffraction patterns of LSCO films deposited at oxygen pressures of 100-300 mTorr. The LSCO layer also have perovskite structure with highly oriented nature. It is noted that the lattice parameter of the LSCO layer decreases with increasing the ambient oxygen pressure. It is known that laser deposition of $Y_1Ba_2Cu_3O_{7-x}$ (YBCO) high Tc supercon-
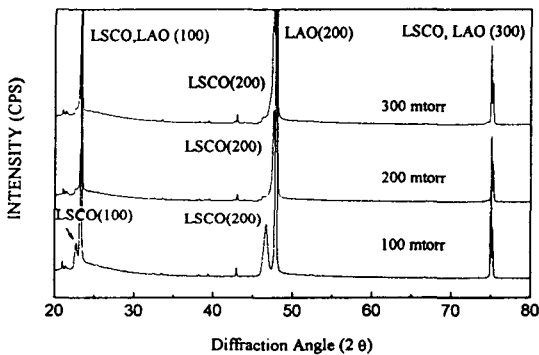
ducting oxide is not the thermally equilibrated process with an oxygen ambient used (typically oxygen pressure of 100-300 mTorr).[15] Consequently, $Y_1Ba_2Cu_3O_7-X$ superconducting films are, in general, annealed at high oxygen pressures during cooling. Similarly, the dependence of the ambient oxygen pressure on the lattice parameter of the LSCO layer (shown in Figure 2) indicates that the LSCO layer is deposited at the growth temperature (650℃) and the oxygen ambient pressures (100-300 mTorr) in non-equilibrium process. Figure 3 also illustrates the effect of post annealing at an oxygen pressure of 400 Torr on the lattice parameter of the LSCO layer. The LSCO layer cooled at an oxygen pressure of 400 Torr exhibited the reduced lattice parameter, compared with the LSCO layer cooled at the same oxygen pressure as the deposition pressure (100 mTorr).

X Pb(Zr,Ti)O_3 (PZT) thin films were further deposited on the LSCO layer. Subse-

Fig. 2. X-ray diffraction patterns of $(La_{0.5}Sr_{0.5})O_3$ CoO_3 films deposited at xoygen pressures of 100-300 mTorr.
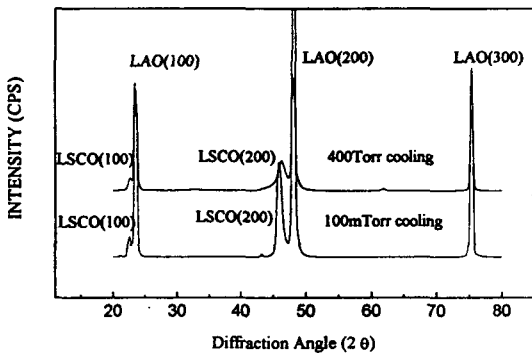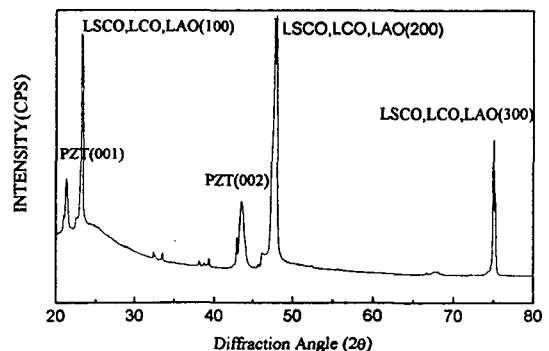

Fig. 3. X-ray diffraction patterns of $(La_{0.5}Sr_{0.5})$ CoO_3 films deposited at an oxygen pressure of 100 mTorr with different oxygen cooling pre

Fig. 4. X-ray diffraction patterns of $LaCoO_3/Pb$ $(Zr_{0.52}Ti_{0.48})O_3/(La0.5Sr0.5)CoO_3$ heterostructure deposited at a substrate temperature of 650℃ and an oxygen pressure of 200 mTorr. The heterostructure was cooled at the oxygen pressure of 400 Torr

quently, LaCoO₃ (LCO) as a channel layer was deposited on the PZT layer to make a LCO/PZT/LSCO heterostructure. Figure 4 shows a x-ray diffraction pattern of the heterostructure. All the layers in the hetero-structure were grown at 650 ℃ and an oxygen pressure of 200 mTorr. Each layer (LCO, PZT and LSCO) in the heterost-ructure was highly oriented with the perov-skite structure. Further, ϕ scan was per-formed on PZT/LSCO heterostructure in order to investigate the in-plane texture of the layers. Figure 5 shows the diffraction peaks obtained by the ϕ scans. The diffrac-tion peaks of LSCO and PZT films are spaced by 90o and no additional peak was observed. In other words, both LSCO and PZT films in the heterostructure have four fold symmetry. This result indicates that
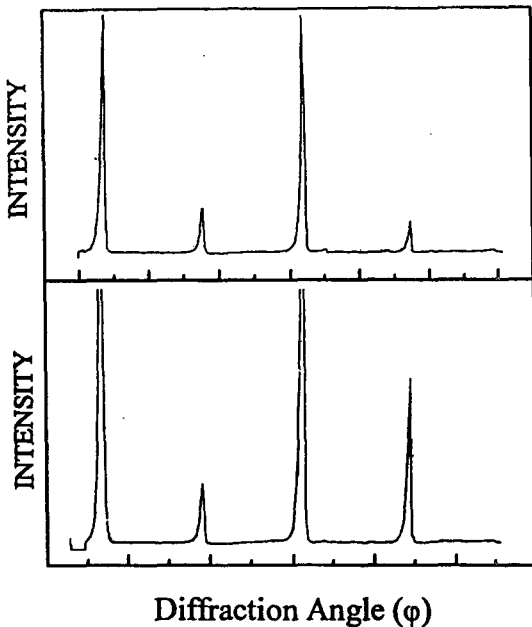
LSCO and PZT films were epitaxially grown. Moreover, the diffraction peaks of LSCO and PZT films are spaced at the same angles (ϕ), which means that LSCO and further PZT films deposited on the substrate were grown epitaxially with a parallel orientation with the substrate. Close lattice matching between LSCO and LaAlO₃ will induce the epitaxial growth of LSCO layer. Subsequently, PZT would be epitaxially grown on the LSCO/ LaAlO₃.

Figure 6 shows polarization-voltage (P-V) hysteresis loops of LCO/PZT/LSCO and

Fig. 5. ϕ scan for (a)(La₀.₅Sr₀.₅)CoO₃ layer and (b) Pb(Zr₀.₅₂Ti₀.₄₈)O₃ layer in Pb(Zr₀.₅₂Ti₀.₄₈)O₃ / (La₀.₅Sr₀.₅)CoO₃ heterostructure.
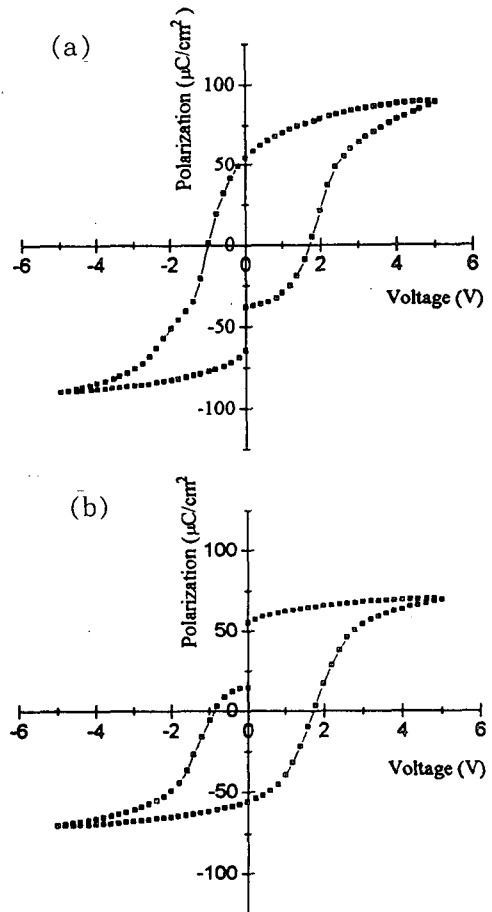
Fig. 6. Polarization-voltage (P-V) hysteresisloops of (a) LaCoO₃/Pb(Zr₀.₅₂Ti₀.₄₈)O₃/(La₀.₅Sr₀.₅)CoO₃ and (b) (La₀.₅Sr₀.₅)CoO₃/Pb(Zr₀.₅₂Ti₀.₄₈)O₃/LaCoO₃ heterostructures.

LSCO/PZT/LCO heterostructures. It is important to obtain large polarization for ferroelectric field effect since the large remnant polarization induces the large ferroelectric field effect in LCO channel layer. The LCO/PZT/LSCO heterostructure had remnant polarization of $70\mu C/cm^2$ at a positively poled state. These remnant polarization values are large, compared with those of PZT films deposited by sol-gel method. The large polarization value of the heterostructure is attributed to the epitaxial nature of the PZT film in the heterostructure. Figure 6 also shows that the P-V hysteresis loop of LCO/PZT/LSCO is not quite symmetric. The remnant polarization of the LCO/PZT/LSCO heterostructure was $17\mu C/cm^2$ at a negatively poled state. In other words, the heterostructure exhibited the relaxation of the remnant polarization at the negatively poled state. It is reported that asymmetric electrode configuration (i. e., Pt/PZT/YBCO) induces asymmetric P-V hysteresis loop.[16] In this LCO/PZT/LSCO heterostructure, LSCO layer was used as an bottom electrode while LCO layer was used as a conducting channel layer as well as a top electrode. This asymmetric electrode configuration is likely to induce the asymmetric hysteresis loop (positively biased) in the LCO/PZT/LSCO heterostructure shown in figure 6 (a). This suggestion is supported by the fact that the positively biased asymmetric hysteresis loop is reverted to the negatively biased hysteresis loop when LSCO/PZT/LCO heterostructure is used, as shown in Figure 6 (b). The asymmetric polarization switching seems to be dependent on the electro-

chemical property of the interface between PZT and the LSCO (or LCO) layers. These heterostructures exhibited high resistivities (10^{10} Ωcm) at the applied voltage of 5 V (larger than the switching voltage).

LCO conducting oxide as a channel layer should have appropriate electrical properties such as resistivity and charge carrier mobility. The LCO layer should have a charge carrier concentration suitable for the current modulation. In other words, the compensating charge in the LCO layer induced by ferroelectric polarization should be the same order as the charge concentration existing the LCO layer. If the resistivity of the LCO layer is too low, i.e., carrier concentration is too high, ferroelectric field effect becomes less effective. The resistivity of the LCO layer was examined by four point probe method. Figure 7 shows the resistivity of the LCO layer in LCO/LaAlO₃. The resistivity of LCO films was in the range of 4-100Ωcm, in which the LCO/LaAlO₃ were cooled at the same oxygen pressure as the deposition pressure (100-300 mTorr). The resistivity decreases with increasing the oxygen pressure, shown in Figure 7. This result is consistent with the dependence of the lattice parameter of the LCO layer on ambient oxygen pressure (figure 2). Moreover, the resistivity of the LCO layer varies with the deposition oxygen pressure while the cooling oxygen pressure was maintained at 400 Torr for all deposition. This indicates that oxygen is not fully incorporated into the LCO layer in post annealing at high oxygen pressure, i.e., cooling at 400 Torr. The heterostructure was cooled at the rate of 10℃/min
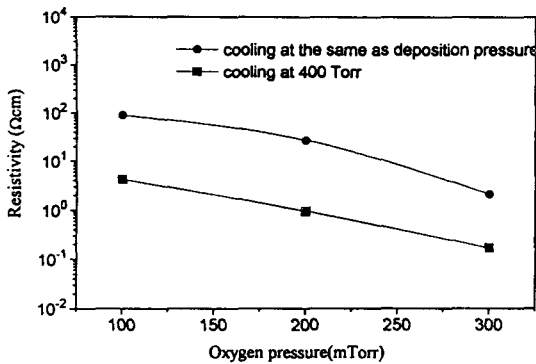
Fig. 7. The resistivity of LaCoO₃ layer in LaCoO₃
/LaAlO₃ deposited at various ambient ox-
ygen pressures. The LaCoO₃ layer was
cooled either at the same as the oxygen
pressure during deposition or 400 Torr.

from the deposition temperature. Therefore, the ambient oxygen pressure during the deposition primarily determines the oxygen content and further the resistivity of the LCO layer. The resistivity of the LCO layer varies in the range of $0.1-100 \Omega cm$ with deposition parameter and cooling oxygen pressure. The carrier concentration of the LCO layer was further estimated from the resistivity of the LCO layer. The LCO layer with the resistivity of $0.1 \Omega cm$ would have the charge carrier concentration of 10 $^{20} cm^{-3}$. It was assumed that the mobility of the LCO is similar to that of $La_{2-x}Sr_xCuO_4$ perovskite conducting oxide.[4] With the charge concentration and the thickness (2000 A) of the LCO layer, the resistance modulation is calculated to be 13% with the PZT layer in the LCO/PZT/LSCO hete-rostructure with a polarization value of 70 $\mu C/cm$ and $17 \mu C/cm$ at the positively and negatively poled states, respectively. The calculation was made with a assumption that zero trap density, zero contact resist-ance. However, the resistance modulation with the polarity of PZT films in the hete-rostructure was not detected within the ac-

curacy of 5%, which can be attributed to poor interface between the LCO and PZT layer. The asymmetric switching behavior is also likely to affect the field effect due to the relaxation at the remnant state. Consequently, a detailed study on thin LCO layer, the interface between the LCO and PZT layers and the contact resistance has to be carried out. Such experiment is in progress and the results will be reported.

CONCLUSION

Epitaxial(La,Sr)CoO₃/Pb(Zr,Ti)O₃/(La,Sr) CoO₃ heterostructures have been grown on LaAlO₃ by pulsed laser deposition for ferro-electric field effect transistor. In the hete-rostructure, LaCoO₃ and (La,Sr)CoO₃ layers were used as a channel layer and elec-trode, respectively. Hysteresis loop obtained from the LCO/PZT/LSCO heterostructure was asymmetric. In other words, the rem-nant polarization was large at the positive-ly poled state while it was small at the negatively poled state. When the LSCO/ PZT/LCO heterostructure is used, the rem-nant polarization at the positively poled state becomes smaller than that at the neg-atively poled state. The resistivity of the LCO layer varies the oxygen pressure dur-ing deposition and cooling. The oxygen am-bient in the deposition process will affect the oxygen content in the LCO layer and further the resistivity of th¹ LCO layer. The current modulation in the LCO layer of the LCO/PZT/LSCO heterostructure was not detected, in which the thickness of LCO layer was 2000 A. This can be attrib-uted to the asymmetric polarization rema-nence or poor interface between the LCO

and PZT layers. More detailed study is need and currently in progress.

ACKNOWLEDGEMENTS

REFERENCES

1. See for example, Proc. of 4th Inter. Symp. on Integrated Ferroelectrics, Ed. C. A. Paz de Araujo, University of Colorado, Monterey, CA, March 1992; Mat. Res. Soc. Proc. 310, Eds. E. R. Myers, B. A. Tuttle, S. B. Desu and P. K. Larsen, Materials Research Society, Pittsburgh, 1993.

2. J. F. Scott and C. A. Paz de Araujo, Science 246, (1989) 1400; S. Dey and R. Zuleeg, Ferroelectrics 108, (1990) 37.

3. S. Sinharoy, H. Buhay, D. R. Lampe and M. H. Francombe, J. Vac. Sci. Technol. A10, (1992) 1554.

4. S. S. Eaton, D. B. Butler, M. Parris, D. Wilson and H. Mcneillie, Proc. of the IEEE Inter. Solid State Conf., San Francisco, California (IEEE, Piscataway, NJ, 1988), p130.

5. R. Womack and D. Tolsch, Proc. of the IEEE Inter. Solid State Conf., San Francisco, California (IEEE, Piscataway, NJ, 1989), p242; R. Moazzami, C. Hu and W. Shepherd, IEEE Electron Device Lett. 11, (1990) 454.

6. R. Ramesh, W. K. Chan, B. Wilkens, H. Gilchrist, T. Sands, J. M. Tarascon, V. G. Keramidas, D. K. Fork, J. Lee and A. Safari, Appl. Phys. Lett. 61, (1992) 1537.

7. J. Lee, L. Johnson, A. Safari, R. Ramesh, T. Sands, H. Gilchrist and V. G. Keramidas, Appl. Phys. Lett. 63, (1993) 27.

8. C. K. Kwok, D. P. Vijay, S. B. Desu, N. R. Parikh and E. A. Hill, Proc. 4th Inter. Symp. Integrated Ferroelectrics, Monterey, California, March 1992, p412.

9. R. Ramesh, H. Gilchrist, T. Sands, V. G. Keramidas, R. Haakenaasen and D. K. Fork, Appl. Phys. Lett. 63, (1993) 3592.

10. J. Lee, R. Ramesh, V. G. Keramidas, W. L. Warren, P. E. Pike and J. T. Evans, Jr., Appl. Phys. Lett. 66, (1995) 1337.

11. D. R. Lampe, D. A. Adams, M. Austin, M. Polinsky, J. Dzimianski, S. Sinharoy, H. Buhay, P. Brabant, Y. M. Liu, Ferroelectrics 133, (1992) 61.

12. S. Sinharoy, H. Buhay, D. R. Lampe and M. H. Francombe, J. Vac. Sci. Technol. A 10, 1554 (1992).

13. C. H. Ahn, J.-M. Triscone, N. Archibald, M. Decroux, R. H. Hammond, T. H. Geballe, O. Fischer, and M. R. Beasley, Science 269, (1995) 373.

14. Y. Watanabe, Appl. Phys. Lett. 66, (1995) 1770.

15. J. Geerk, G. Linker and O. Meyer, Materials Science Reports 4 (1989) 193.

16. J. Lee, A. Safari and R. L. Pfeffer, Appl. Phys. Lett. 61, (1992) 1643.